IEEE Access
Multidisciplinary | Rapid Review | Open Access Journal

Received January 23, 2021, accepted February 1, 2021, date of publication February 9, 2021, date of current version February 18, 2021.

*Digital Object Identifier 10.1109/ACCESS.2021.3058239*

# A Flexible Dual-Band Rectenna With Full Azimuth Coverage

**SANDHYA CHANDRAVANSHI[1], (Member, IEEE), KRANTI KUMAR KATARE[2], (Member, IEEE), AND M. J. AKHTAR[2], (Senior Member, IEEE)**

[1]Department of Materials Science Program, IIT Kanpur, Kanpur 208016, India
[2]Department of Electrical Engineering, IIT Kanpur, Kanpur 208016, India

Corresponding author: Sandhya Chandravanshi (sandhyachandravanshi.iitk@gmail.com)

This work was supported by the Indian Institute of Technology, Kanpur, India.

**ABSTRACT** This paper presents a novel cylindrical shaped dual-band flexible rectenna capable of harvesting RF energy from number of RF sources available in the entire azimuth plane. The proposed configuration is an array of four identical dual-band rectenna subsystems, printed on the lightweight flexible substrate. Here, each rectenna subsystem comprises of a dual-ring shaped dual-band monopole antenna and a dual-band rectifying circuit. The designed topology is good for popular bands of LTE 1.8 GHz and Wi-Fi 2.45 GHz. The robustness of the designed antenna in the proposed cylindrical shaped rectenna is also verified by testing it for different bending angles in the H-plane by simulation as well as measurement. The bending performance is tested for the antenna using S11 and farfield radiation pattern. Further, for extracting maximum RF signals in the entire azimuth plane, these four identical antennas are backed by a wide-band artificial magnetic conductor (AMC) placed in the inner region of the cylinder. The fabricated single rectenna unit is capable of converting power with 40% efficiency at very low input RF power −12 dBm. Finally, the overall rectenna array is fabricated and validated through measurements using two different test antennas as a RF sources in the real environment of lab. The proposed light weight, rectenna printed on a flexible substrate can extract RF signals from a number of randomly distributed RF sources simultaneously, while maintaining the overall compact configuration.

**INDEX TERMS** Azimuth coverage, dual-band, flexible substrate, light-weight, monopole antenna, rectenna, rectifier.

## I. INTRODUCTION

The increasing demand of light-weight and compact harvesting systems have fostered researchers to develop the rectenna on a flexible substrate. Here, the major challenge of designing the flexible rectenna system is the performance variation with the bending effect specially for the antenna. Previously the bending effect on a patch antenna in terms of matching and radiation pattern has been analyzed in detail [1]. A rectangular single band patch antenna on a textile substrate using Silver-copper-nickel plating with 4.4 dBi gain was reported [2]. In order to enhance the gain of antenna on any flexible substrate material, the array of antennas with the AMC backed structure was proposed in [3]. In this work, a Foam-backed paper was used as a substrate, on which silver ink has been used for printing the conductive design of 3 × 2 array of antenna with 7 dBi gain. A single band array of 3 × 3, loop antenna on a Parylene-C substrate has been reported in [4]. From these works, it can easily be predicted that the considerable research effort has been placed in order to achieve high gain on flexible antenna system. Apart from aforementioned antenna structures, numerous rectenna designs on flexible substrate have also been reported in literature. The idea of wide band or multi band rectenna design was also implemented on flexible rectenna system to get high efficiency from the overall system. A wide band hybrid rectenna system on flexible PET substrate was reported in [5]. Another approach on a Kapton substrate using inkjet printing was reported in [6]. This configuration was comprised of an UWB rectifying circuit with the efficiency greater than 33% for mentioned frequency range. In order to obtain light weight rectenna system, various architectures based on paper

The associate editor coordinating the review of this manuscript and approving it for publication was Bilal Khawaja.

substrate have been reported [7]–[11]. Recently, an efficient flexible rectenna system reported in [11] tested for wristband application. Most of these reported works were focused on a single rectenna system, where receiving power was obtained from a single direction only. In order to obtain more converted power, different types of rectenna array have been designed on a rigid substrate [12]–[15]. Moreover, while using the array of rectenna system on rigid substrate has a constraint of angular coverage with the compact size, in [16]–[18] wide angular coverage is reported. The work done in [18] is reported for an angular coverage with antenna fabricated on flexible substrate while rectifiers are connected via butler matrix with the receiving antenna. In addition with array configuration, a multiband approach in order to process signal from multiple sources simultaneously, which results into enhancement of overall converted power has also been proposed [5], [6], [19]–[22].

From above discussion it can be inferred that there is still need of light-weight flexible rectenna, capable of extracting RF energy from multiple RF sources, distributed randomly in the space. This type of requirement is achieved here by utilizing an array of four rectenna subsystems oriented towards four orthogonal directions. Here, each rectenna is obtained by integrating a dual-band dual-ring shaped monopole antenna with a dual-band rectifying circuit. The stable performance of dual-ring shaped monopole antenna for different bending angles is also validated through both simulation and measurement. Finally, the complete novel rectenna system is printed on a single flexible substrate and folded to from a cylindrical shape, which makes it more compact. The available space inside cylindrical shaped rectenna is further utilized by incorporating a wide-band AMC surface in this region. This AMC enhances the gain of each dual-ring shaped monopole antenna by making the antenna unidirectional in both of the operating frequency bands. The rectenna system is novel in terms of its specific design, where all the elements are placed in a compact cylindrical system. The dual-band nature, flexible substrate, light weight and integration in a single system shows the applicability of the proposed configuration.

## II. DESIGN GUIDELINES AND SYSTEM CONFIGURATION

In the proposed cylindrical rectenna system, four identical rectenna subsystems each comprised of a dual-ring shaped dual-band monopole antenna and a rectifying circuit are utilized. The rectifying circuit is basically composed of a rectifier circuit with a dual-band matching unit. The entire structure is backed by a wide-band artificial magnetic conductor (AMC) surface. The design of each element of the proposed cylindrical rectenna system is elaborated in this section.

### A. DUAL-RING SHAPED MONOPOLE ANTENNA

The proposed dual-ring shaped monopole antenna with its design dimensions is shown in Fig. 1(a). This antenna is basically comprised of two annular rings with the centres of $C_{in}$, $C_{out}$ and the radius of $r_{in}$, $r_{out}$ correspondingly. These rings

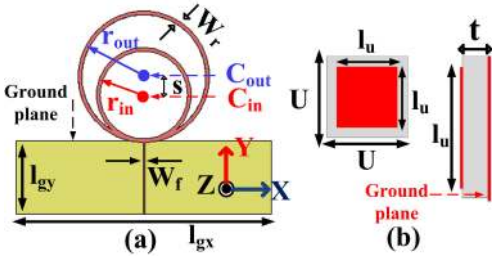


**FIGURE 1.** (a) Topology of the dual-ring shaped dual-band antenna ($r_{in}$ = 12, $r_{out}$ = 17, $S$ = 5, $W_r$ = 1, $W_f$ = 0.45, $l_{gy}$ = 20, $l_{gx}$ = 70) (b) Unit cell of the AMC structure ($l_u$ = 29, $U$ = 31, $t$ = 8) all dimensions in mm.

are fed through a single microstrip line with the impedance of 50 Ω and backed by a partial ground plane. The perimeter of each ring is equaled to the operating wavelength of antenna and hence dual-ring shaped configuration is mainly responsible for obtaining the dual-band performance. Therefore, inner and outer rings of this antenna are mainly contributing two operating frequency bands individually. In order to couple RF signals to these dual-rings of antenna using a single microstrip line, the center of inner ring ($C_{in}$) is shifted in the −Y direction by a distance of $S$ from the center of outer ring ($C_{out}$). Therefore, this approach enable the whole antenna to radiate via feeding through a single microstrip line, as shown in Fig. 1(a). This location of inner ring facilitates dual-band performance with the adequate matching in both of the operating frequency bands. The performance of this antenna with different bending angles (30° to 90°) in the H-plane is also discussed in the later Section. It will be shown that performance of the proposed dual-ring shaped antenna in terms of both matching and radiation characteristics is highly stable for a large range of bending angles, therefore suitable to design cylindrical shaped rectenna system.

### B. ARTIFICIAL MAGNETIC CONDUCTOR (AMC)

In the proposed rectenna system, the entire assembly of four dual-ring shaped antennas along-with their corresponding rectifying circuits are backed by a wide-band artificial magnetic conductor (AMC) surface. This AMC surface works as a reflecting surface and facilitates low profile structure due to its inherent 0° phase reflecting characteristics. The AMC utilized in this configuration is basically an array of unit cells (dimension: $U \times U$), where each unit cell is comprised of a squared shaped metallic structure (dimension: $l_u \times l_u$) backed by a ground plane, as depicted with design dimensions in Fig. 1(b). In order to cover both operating frequency bands of the proposed rectenna system, the bandwidth of 0° phase reflection characteristics of the AMC unit cell is broadened here by utilizing a space of $t = 8$ mm between the top (square shaped metal structure) and the bottom (ground plane) layers. This wide-band AMC can easily operate for both frequency bands of the rectenna system. Since, the proposed rectenna system is designed on the thin flexible substrate, both operating frequency bands of the antenna along-with rectifying

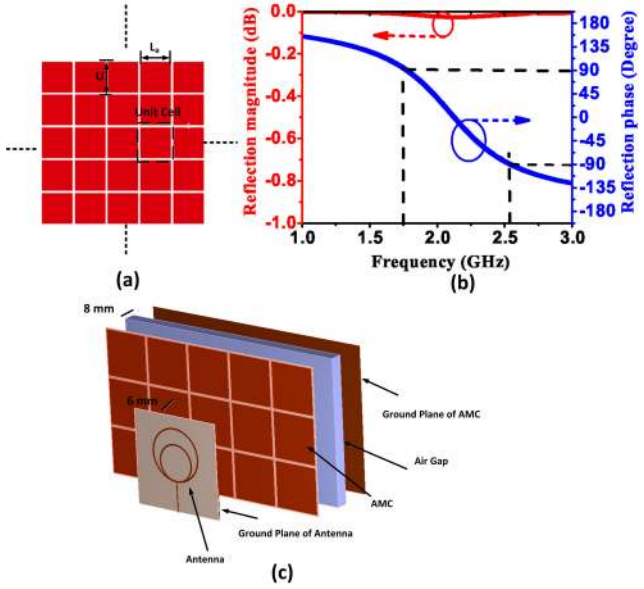


**FIGURE 2.** (a) Designed AMC (b) Reflection characteristics of unit cell of the AMC structure in terms of magnitude and phase (c) The layout of the proposed dual-ring shaped antenna including AMC.

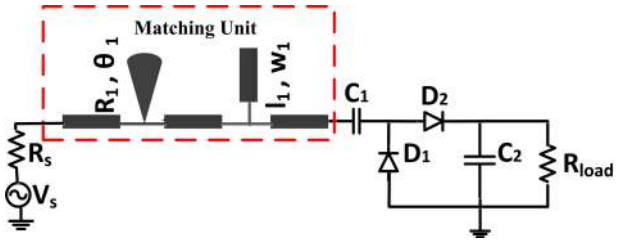


**FIGURE 3.** The schematic of the proposed rectifying circuit, in this schematic the matching unit consists of radial stub ($R_1 = 4.3$, $\theta_1 = 110$) and an open stub ($l_1 = 12.2$, $w_1 = 0.61$, capacitors $C_1 = C_2 = 47$ pF.

circuit would be inherently narrow-bands. Therefore, in lieu of using a dual-band, a wide-band AMC surface is adopted in the proposed configuration in order to ensure satisfactory operation of the proposed rectenna system in both of the operating frequency bands. Moreover, the wide-band topology of the AMC unit cell (8 mm space between top and bottom layers) basically utilizes the unused space inside the cylindrical cavity, hence seems to be suitable for this specific configuration of the rectenna system. Finally, designed AMC would be a periodic distribution of metallic patches shown in Fig.2(a). The reflection characteristics of the single unit cell of this AMC in terms of magnitude and phase is depicted in Fig. 2 (b). It is found the reflection magnitude for the incident EM waves impinging on this unit cell is quite high in the in-phase ($-90°$ to $+90°$) operating frequency band starting from 1.75 GHz to 2.6 GHz. So, for this particular case the bandwidth of the AMC would be 850 MHz (from 1.75 GHz to 2.60 GHz). In this frequency range, magnitude of reflection coefficient is also quite high (around 0 dB). This band is certainly comprised of the operating frequency bands of the rectenna system.

The proposed topology mainly consists a 3-layered structure Fig. 2(c), where the first layer accomplished of a receiving unit, comprising a dual ring monopole antenna and the rectifier circuit backed by a metallic ground plane. This layer is designed and afterwards fabricated on a Polyimide based flexible substrate. The second layer consist of metallic patch structure with periodically spaced patches printed over the same Polyimide based flexible substrate. The second layer is to be placed after a 6 mm of airgap from the first layer, this gap was optimized for the best performance of the rectenna. The last or third layer of the structure is the metallic ground plane which is separated by an air gap from second layer. The combination of the second layer and third layer is basically known as an Artificial Magnetic Conductor (AMC) structure. Here, air gap (8 mm) between the second layer and the third layer is optimized in order to obtain wider bandwidth of the AMC structure. This three-layer structure (shown in figure Fig. 2(c) corresponds to a single rectenna configuration. Finally, the designed rectenna topology is obtained here by utilizing four same kind of aforementioned rectenna structure and then folded it to from a cylindrical body.

### C. DUAL-BAND RECTIFYING CIRCUIT

This sub-section mainly focus on detailed design of the rectifying circuit used for proposed rectenna system. The rectifying circuit is most important section of any rectenna system. The RF to dc conversion efficiency of any rectifying circuit is the function of operating frequency, input RF power, substrate material, output dc load and diode. The rectifying circuit designed for this work consists of a dual band matching unit, a rectifier unit and load resistor. The rectifier mainly accommodate commercially available schottky diodes (SMS-7630, with a very low value of forward voltage $V_f = 60$ to 120), and lumped capacitors. The main aim of the proposed circuit is to optimize efficiency for the low input RF power value (around $-20$ dBm), so this particular diode is chosen here for this work. The components used here in order to get dual band are mainly radial and open stubs, other micro-striplines are connecting lines as depicted in Fig. 3. The values of the length, width, radius and angle of the open and radial stubs are shown in the caption of Fig. 3. The presented circuit in this figure is firstly optimized and designed using ADS circuit simulator software.

## III. RESULTS AND DISCUSSION

The results of the proposed configuration is illustrated in this section.

### A. DUAL-RING SHAPED MONOPOLE ANTENNA WITH AMC SURFACE

The dual-ring shaped monopole antenna is basically comprised of two circular rings each is responsible for different frequency bands. The location of inner ring plays a vital role

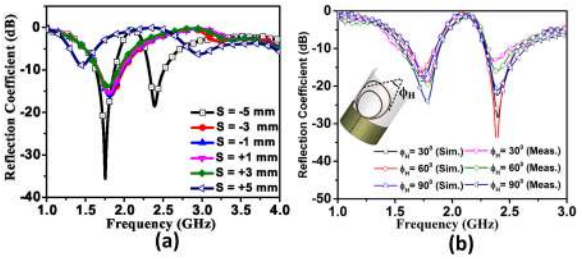


**FIGURE 4.** Parametric analysis of the designed antenna (a) Matching characteristics of the dual-ring shaped dual-band antenna for different locations ($S$) of the inner ring (b) matching characteristics of the dual-ring shaped dual-band antenna for different bending angles ($\phi_H$) in the H-Plane.

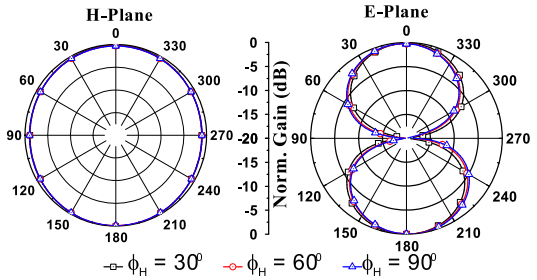


**FIGURE 5.** Simulated radiation characteristics of the dual-ring shaped dual-band antenna for different bending angles ($\phi_H$) in the H-Plane.

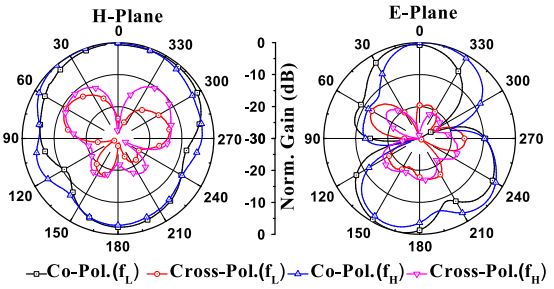


**FIGURE 6.** Measured radiation patterns of the dual-ring shaped dual-band antenna at the centers ($f_L$ = 1.8 GHz and $f_H$ = 2.45 GHz) of both of the operating frequency bands.

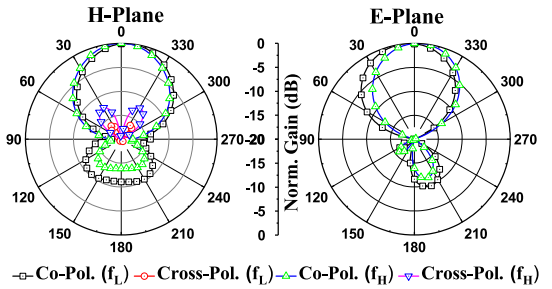


**FIGURE 7.** Simulated radiation characteristics of the dual-ring shaped dual-band antenna when backed with AMC.

to achieve the adequate matching in both of the operating frequencies. In order to verify this concept, matching characteristics of this antenna for different location ($S$) of inner ring is depicted in Fig. 4 (a). From this figure it can easily be observed that for the extreme locations ($S = -5$ mm and $S = +5$ mm) of the inner ring, dual-band performance is obtained. Whereas for other locations ($-5 < S < +5$), due to the week coupling between microstrip feed line and the inner ring, only single lower frequency band corresponding to the outer ring is obtained. Since, the best matching performance in both of the operating bands is obtained for the inner ring location of $S = -5$ mm, hence utilized in this configuration.

The analysis is further carried out to show the robustness of the proposed monopole antenna with different bending angles in the H-plane. The matching characteristics and normalized radiation pattern (co-polar radiation patterns in the both H and E-planes) of this antenna for different bending angles ($\phi_H = 30°$ to $\phi_H = 90°$ ) are shown in Fig. 4 (b) and Fig. 5, respectively. It is interesting to find that performance of the proposed antenna is highly stable for a large range of bending angles. It is to be mentioned here that the cross-polar radiation component remains in the tolerable limit for all the bending angles of the antenna, however does not depicted here for brevity. Since, the main objective in the designing of the proposed rectenna system is to bend the monopole antenna in its H-plane only, hence the bending effect of this antenna is analyzed in the same H-plane only. Moreover, radiation patterns in both of the frequency bands are found to be stable for different bending angles of antenna in the H-plane, for brevity these patterns are depicted at a single frequency ($f_H = 2.45$ GHz) only. The measured radiation patterns of the stand-along dual-ring shaped monopole antenna without bending at both the lower ($f_L$) and the upper ($f_H$) frequency bands are depicted in Fig. 6. After designing and testing of dual-ring dual band antenna, it is backed with the AMC. For the verification of the concept that the AMC makes the pattern to be an unidirectional, the simulated and measured radiation characteristics are plotted in Fig. 7 and Fig. 8, respectively. It can be observed from these figures that the measured results are in good agreement with simulation results. It is to be noted that in the real fabricated rectenna system, this antenna makes an angle of $\phi_H = 55°$ from the centre of the cylindrical rectenna system. Therefore, for ensuring the performance of the antenna for this particular bending angle in the H-plane, the measured radiation patterns of the antenna with bending angle of $\phi_H = 55°$ at both of the operating frequencies is shown in Fig. 9.

A 3D radiation patterns of the proposed configuration at the two operating frequencies (Fig. 10(a) at 2.45 GHz and Fig. 10 (b) at 1.8 GHz) are shown. These patterns are obtained by exciting each antenna individually. It is to be mentioned that for better visibility, 3D patterns are shown while exciting three antennas one after another only (since fourth antenna is at the back side of figure so the corresponding radiation pattern is less visible and hence not included here for brevity). These patterns justify performance of the overall structure by covering the entire azimuth plane. Here, all four antennas are radiating in the broadside direction which assures the

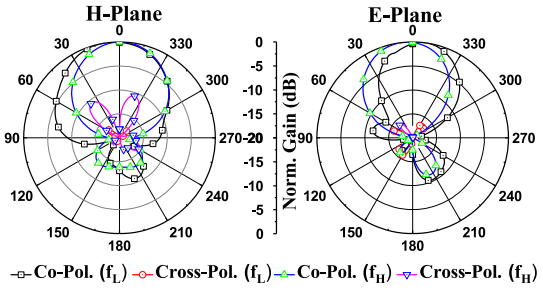


**FIGURE 8.** Measured radiation characteristics of the dual-ring shaped dual-band antenna when backed with AMC.

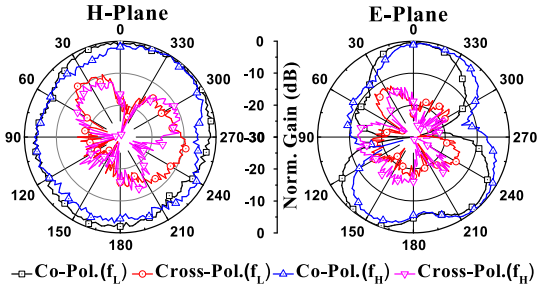


**FIGURE 9.** Measured radiation patterns of the dual-ring shaped dual-band antenna with bending in the H-plane ($\phi_H = 55°$) at the centers ($f_L = 1.8$ GHz and $f_H = 2.45$ GHz) of both of the operating frequency bands.

full azimuth plane coverage by the array while exciting them simultaneously.

### B. MAJOR RESULTS OF RECTIFYING CIRCUIT

The selection of the optimized load value for a multiband rectifier circuit is quite complicated process. So, in this work the source pull technique of the ADS software is adopted in order to simplify the whole process. Firstly, for both operating frequencies, the load value of 2.5 kΩ is selected. Afterwards, while considering this already known value of the load, the matching unit is designed. For getting the matching characteristics of the proposed rectifying circuit, the Large Signal S-parameter (LSSP) method of ADS software is opted here. On the other hand for the measurement the fabricated structure is connected to the VNA via a SMA connecter. The recorded values of the reflection coefficients are plotted, as shown in Fig. 11 (a) at various input RF power levels. It can be observed from this figure that the two bands at around 1.8 GHz and another at 2.45 GHz are obtained here. The simulated and measurement results are well matched with each other, however the minor disagreement may be due to the soldering of the lumped components. In this work as the substrate is very thin these effects would be dominated at some temperature conditions.

After, obtaining the operating frequency points and the load resistance value, efficiency of the rectifying circuit would be calculated by measuring the output dc voltage at the load resistor. Firstly, the simulated output dc voltage at 2.5 $k\Omega$ is obtained later on the efficiency at the corresponding

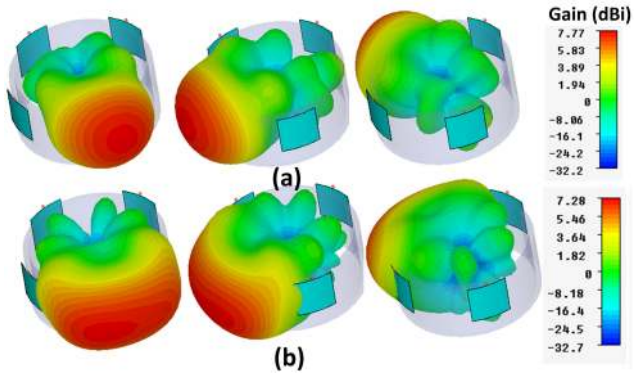


**FIGURE 10.** 3D radiation patterns of the proposed configuration at (a) 2.45 GHz (b) 1.8 GHz.

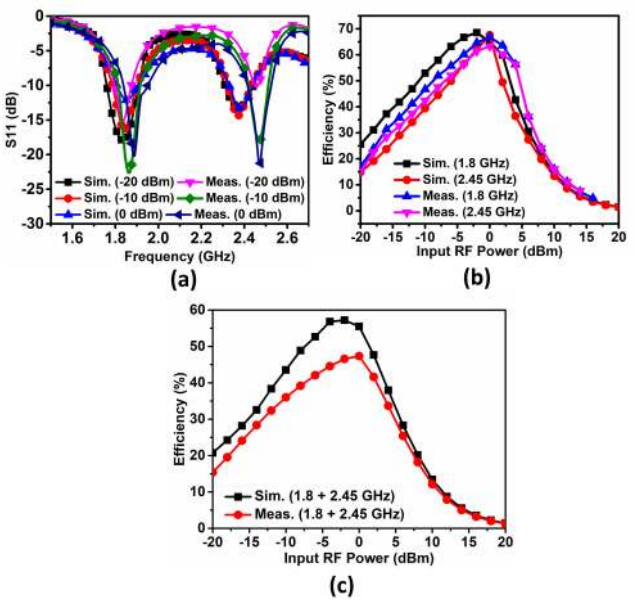


**FIGURE 11.** Simulated and measured results of the rectifying circuit (a) The S11 of the proposed rectifying circuit, the simulated and measured RF to dc conversion efficiency of the rectifying circuit (b) for individual frequency (c) for dual tone method.

frequency points is calculated using the formula given in Eq. (1), where $P_{DC}$ is the calculated DC power at the optimized load value and $P_{IN}$ is the RF power available at the input of the rectifying circuit.

$$\text{Efficiency } (\%) = \frac{P_{DC}}{P_{IN}} \times 100 \tag{1}$$

For the measurement, the input RF power is fed using a signal generator which is connected to the rectifying circuit via a SMA connector and a coaxial cable. The efficiency is calculated and also plotted as a function of input power, as shown in Fig. 11 (b). A maximum simulated and measured efficiency of 69% and 68% are achieved for an input RF power value of −2 dBm and 0 dBm, respectively at 1.8 GHz of operating frequency. It can be noted from this figure that for 2.45 GHz, the simulated and measured value of efficiencies are 67% and 64% are obtained, respectively.

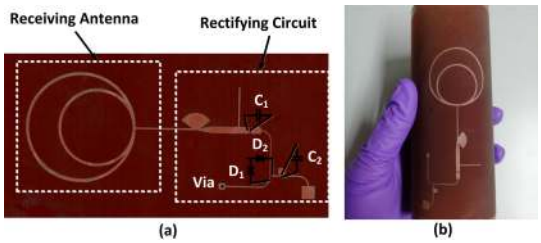


**FIGURE 12.** Fabricated structures (a) representing antenna and rectifying circuit with SMT components (b) flexible rectenna structure.

The proposed rectifying circuit is designed mainly for the low RF power values, where better efficiency is obtained. At very low RF power such as −20 dBm the simulated and measured efficiency for 1.8 GHz and 2.45 GHz of frequency are 26% and 17% are achieved, respectively. This assures that the circuit is well suitable for the low power application. Around, 0 dBm input RF power value, the RF to dc conversion efficiency starts decreasing slowly, which may happen due to the saturation point of the output dc voltage reached. This usually happens, when the break down voltage of the used diode is approached.

Afterwards, for verification of the proposed circuit towards the ability to multiple signal receiving efficiency the two tone efficiency is calculated, represented in Fig. 11(c). For this firstly the simulation results are obtained by considering two tone (at 1.8 and 2.45 GHz) RF power source at the input port of the dual band rectifier circuit. from here the converted dc voltage is recorded and then RF to dc conversion efficiency is calculated. Afterwards, to obtain measured data from the fabricated circuit two signal generators via a power combiner fed to the input port of the rectifier circuit and then RF to dc conversion efficiency is calculated from the obtained dc voltage across a 2.5 kΩ load value. The RF to dc conversion efficiency obtained for dual tone signals assures that the designed rectifier can work efficiently for multiple signals at a time. The conversion efficiency in this case is low as compare to the single tone operation due to high received power.

## IV. RECTENNA SYSTEM

Fig. 12 (a) illustrates the finally designed fabricated rectenna sub-system, which is a combination of the receiving dual-ring shaped monopole antenna and the rectifying circuit. The antenna and the rectifying circuit are both integrated over the same substrate, in order to make the system more reliable. The designed rectenna unit is very flexible which can be easily predicted from Fig. 12 (b). The measured efficiency of the single rectenna unit is shown in Fig. 13. For getting the integrated system of four identical rectenna units the dc combining approach [23] is adopted here, as shown in Fig. 14. The concept of parallel additive method is used in order to obtain high converted power. In the proposed method the optimized load value is calculated from the load value of the single rectifying circuit, Eq. 2. Here, N would be taken as 4, thus the calculated load for overall architecture would be as 0.625 kΩ. In this adopted parallel topology the obtained voltage from each branch would be nearly equal while the current adds up at the load, resulting in to enhancement in the converted power.

**TABLE 1.** Measured values of output DC voltages for line of sight transmitting antennas at 1.8 GHz and 2.45 GHz.

| Distance/ Power at S.G | P=0 | P=4 | P=8 | P=12 | P=16 | P=20 |
|---|---|---|---|---|---|---|
| 1.8 GHz | | | | | | |
| 20 cm | V = 0.041 | V = 0.09 | V = 0.188 | V = 0.362 | V = 0.65 | V = 1.2 |
| 40 cm | V = 0.015 | V = 0.041 | V = 0.093 | V = 0.185 | V = 0.35 | V = 0.65 |
| 2.45 GHz | | | | | | |
| 20 cm | V = 0.021 | V = 0.085 | V = 0.17 | V = 0.32 | V = 0.45 | V = 0.98 |
| 40 cm | V = 0.003 | V = 0.0211 | V = 0.0843 | V = 0.152 | V = 0.25 | V = 0.55 |

**TABLE 2.** Measured values of output DC voltage for orthogonally oriented transmitting antennas at 1.8 GHz 2.45 GHz.

| Distance/ Power at S.G | P=0 | P=4 | P=8 | P=12 | P=16 | P=20 |
|---|---|---|---|---|---|---|
| 1.8 GHz | | | | | | |
| 20 cm | V = 0.038 | V = 0.09 | V = 0.173 | V = 0.322 | V = 0.56 | V = 0.98 |
| 40 cm | V = 0.015 | V = 0.038 | V = 0.088 | V = 0.165 | V = 0.35 | V = 0.6 |
| 2.45 GHz | | | | | | |
| 20 cm | V = 0.02 | V = 0.065 | V = 0.123 | V = 0.222 | V = 0.457 | V = 0.85 |
| 40 cm | V = 0.001 | V = 0.021 | V = 0.063 | V = 0.185 | V = 0.24 | V = 0.46 |

$$Load = (R_{load})/N \tag{2}$$

In order to obtain this efficiency, the transmitting horn antenna is fed using signal generator via a coaxial cable. The received power by the receiving antenna is measured using a spectrum analyzer. In this setup, we have fixed the power of signal generator at some RF power value and the distance between transmitter antenna and the receiver antenna is to be varied from 100 cm to 20 cm. At every distance point the received power using spectrum analyzer has been measured at both the operating frequencies. This approach, facilitates the wide area coverage to antenna as the beam width of the antenna would not be affected. The inner most layer of this cylindrical system is actually the ground layer of the AMC, afterwards the AMC at 8 mm air gap has been placed. Afterwards, the array of four rectennas has been placed followed by the ground of rectenna at the 6 mm distance from the AMC. (single unit is depicted in Fig. 2 (c)). Now, the fabricated prototype of the rectenna array is represented in Fig. 15 (a), this is a finally designed cylindrical system. For making the compact rectenna array, it has been bend at the already tested angle. The output of each rectenna unit is connected to the adjacent rectenna unit, which is finally feed to the dc output load of 0.625 kΩ. Further, the dc lines are designed here to be

**TABLE 3. Comparison of the proposed work with other related designs.**

| Ref. | Freq. Band (GHz) | Available RF Power (dBm) | Eff. (%) | Size ($mm^2$) | Load (kΩ) | Weight (gm) | Angle Coverage | Substrate |
|---|---|---|---|---|---|---|---|---|
| [7] | 2.45 | 0 dBm | 40 | 50 × 11 | 1 | NA | Monopolar Pattern | LCP |
| [10] | 0.79-0.96 | 6 $\mu W$ / $cm^2$ | 57 | 110×110 | 2 | 6 | NA | paper |
| | 1.71-2.69 | | | | | | | |
| [16] | 1.8 | -20 dBm | 21.1 | 56×98 | 6 | NA | Omnidirectional (0-360°) | Rogers 4003 |
| [17] | 2.45 | 0.5 $\mu W$ / $cm^2$ | 35.2 | 226×337 | NA | NA | Broadside | FR4 |
| [21] | 1.7-1.9, | -10 dBm | 32 | 90×45 | 6.7 | NA | Monopolar Pattern | FR4 |
| | 2.25-2.46 | | | | | | | |
| This | 1.8 | -12 dBm | 40 | 92×70 | 2.5 | 9.5 | Azimuth Plane | Polyimide |
| Work | 2.45 | | 33 | | | | | |

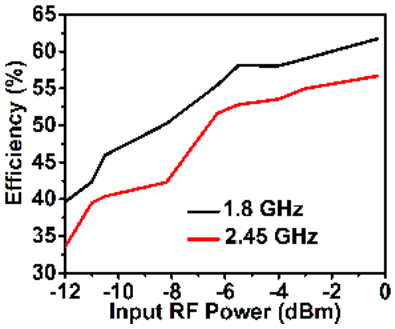


**FIGURE 13. Measured efficiency of the single unit rectenna.**

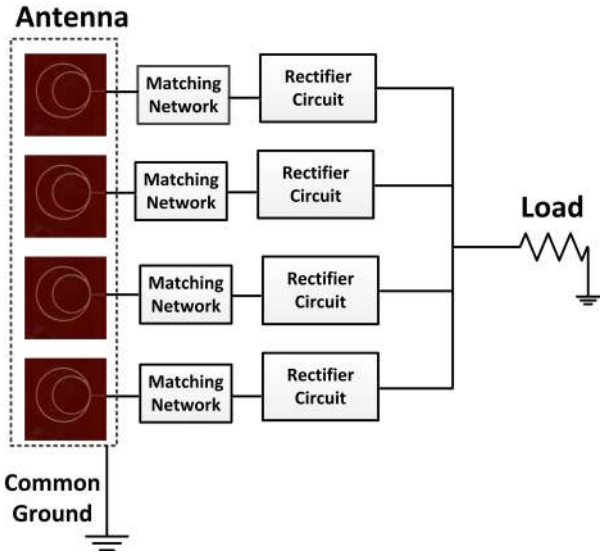


**FIGURE 14. Description of the proposed rectenna architecture.**

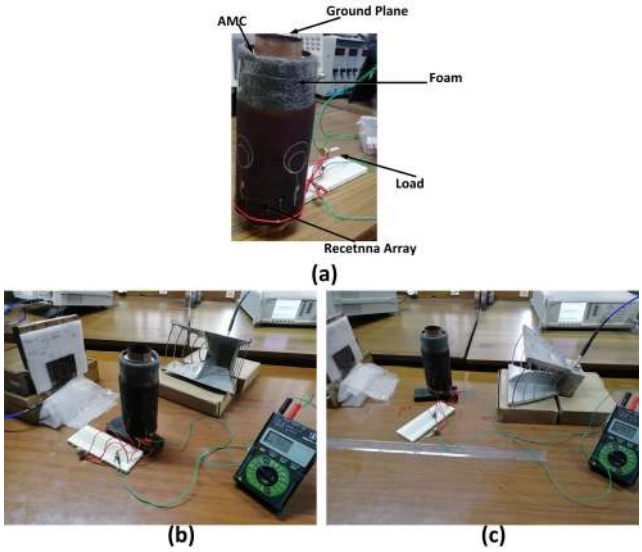


**FIGURE 15. Description of the overall structure and measurement setup (a) closed view of cylindrical rectenna. Measurement setup for the fabricated rectenna array (b) both transmitting antennas are at 90° to each other (c) once the transmitting Horn antenna and fabricated monopole antenna are in line of sight.**

very thin using wires for connecting four rectenna units are to yield minimal inductance to the load.

Afterwards, the measurement of the designed rectenna array system is carried out, which represented in Fig. 15. Now, to justify the design phenomenon of the proposed structure we have used two setups in which RF signal can be received from two different directions. In first setup, the transmitting antennas are kept at 90° to each other as shown in Fig. 15 (b). In second setup the two transmitting antennas are placed at the line of sight to each other or at 180° to each other as depicted in Fig. 15 (c). For both setups, the output dc voltages (V in mV) are measured using multimeter at the optimized load resistance by varying the power (P in dBm) from signal generators for two different distance (20 cm and 40 cm) between the transmitter and the receiver, which are represented in Tables 1 and 2. It can be noted from these tables that in both conditions quit good amount of power is converted into DC by the designed configuration. Which assures the power transmission and conversion of the proposed topology from the multiple directions.

In order to compare the proposed work with previously reported works, we have gone through similar kind of work based on non-flexible and flexible substrate. The comparison is listed in Table 3. From this comparison, we can easily conclude that the efficiency obtained using proposed rectenna system is quite good at the lower power region. In addition to this, the proposed system is dual band which can extract power from the two RF sources operating at two different frequencies. Moreover, our proposed rectenna system is quite compact and light weight as it is designed over a flexible substrate, which can be easily implemented in any microwave power transfer system. The work carried out in all these research papers is undoubtedly very good. However, the work

proposed in our manuscript is also novel in many aspects, especially in terms of application. In this work, our aim is to report the architecture which could be implemented in the low power devices. In order to fulfil this requirement, we have designed a very lightweight (38.18 gm) compact structure, which can receive signals from all directions existing in the azimuth plane. The weight of a single rectenna unit used in our configuration is only 9.5 gm. Some of the references in the table also receives signal from large angular direction and researchers have provided the deep knowledge with a very novel design, however, the structures are made on rigid substrate with a single frequency response, which differentiate our proposed work from these reported works. The references [10] and [21] has reported very novel efficient dual band structure however, in [21] the designed structure is not on a flexible substrate and can receive signal mainly from two opposite directions (due to the monopolar pattern). All these aforementioned differences make our design new as per our knowledge and quite efficient with compact and lightweight design. In addition, with this, our design can efficiently receive signal from multiple directions for two popular frequency sources.

## V. CONCLUSION

In this paper, a cylindrical shaped dual-band rectenna system capable of extracting RF energy from a number of RF sources available in the wide coverage area has been presented. The proposed configuration is an array of four identical dual-band rectenna units printed on the lightweight flexible substrate. The rectenna system is basically oriented towards the entire azimuth plane by keeping four rectenna subsystems each with 90° steps. Here, each rectenna subsystem comprises of a dual-ring shaped dual band monopole antenna and the dual band rectifying circuit. The robustness of this antenna in the proposed cylindrical system was also verified by testing it for different bending angles in the H-plane. Further, for extracting maximum RF signals in the entire azimuth plane, these four identical antennas were backed by a wide-band artificial magnetic conductor (AMC) placing in the inner region of the cylinder. A single rectifying circuit of the proposed system was obtained here by combining a matching unit and a rectifier circuit. Finally, the overall rectenna system has been fabricated and validated through measurements using two different test antennas as a RF sources in the real environment of lab. The proposed light weight integrated rectenna system printed on a flexible substrate can extract RF signals from a number of randomly distributed RF sources simultaneously, while maintaining the overall compact configuration.

## REFERENCES

[1] L. Song and Y. Rahmat-Samii, "A systematic investigation of rectangular patch antenna bending effects for wearable applications," *IEEE Trans. Antennas Propag.*, vol. 66, no. 5, pp. 2219–2228, May 2018.

[2] I. Locher, M. Klemm, T. Kirstein, and G. Troster, "Design and characterization of purely textile patch antennas," *IEEE Trans. Adv. Packag.*, vol. 29, no. 4, pp. 777–788, Nov. 2006.

[3] B. S. Cook and A. Shamim, "Utilizing wideband AMC structures for high-gain inkjet-printed antennas on lossy paper substrate," *IEEE Antennas Wireless Propag. Lett.*, vol. 12, pp. 76–79, 2013.

[4] J. Maeng, B. Kim, D. Ha, and W. J. Chappell, "Parylene interposer as thin flexible 3-D packaging enabler for wireless applications," *IEEE Trans. Microw. Theory Techn.*, vol. 59, no. 12, pp. 3410–3418, Dec. 2011.

[5] A. Collado and A. Georgiadis, "Conformal hybrid solar and electromagnetic (EM) energy harvesting rectenna," *IEEE Trans. Circuits Syst. I, Reg. Papers*, vol. 60, no. 8, pp. 2225–2234, Aug. 2013.

[6] J. Kimionis, A. Collado, M. M. Tentzeris, and A. Georgiadis, "Octave and decade printed UWB rectifiers based on nonuniform transmission lines for energy harvesting," *IEEE Trans. Microw. Theory Techn.*, vol. 65, no. 11, pp. 4326–4334, Nov. 2017.

[7] A. Eid, J. G. D. Hester, J. Costantine, Y. Tawk, A. H. Ramadan, and M. M. Tentzeris, "A compact source–load agnostic flexible rectenna topology for IoT devices," *IEEE Trans. Antennas Propag.*, vol. 68, no. 4, pp. 2621–2629, Apr. 2020.

[8] V. Palazzi, C. Kalialakis, F. Alimenti, P. Mezzanotte, L. Roselli, A. Collado, and A. Georgiadis, "Performance analysis of a ultra-compact low-power rectenna in paper substrate for RF energy harvesting," in *Proc. IEEE Topical Conf. Wireless Sensors Sensor Netw. (WiSNet)*, Jan. 2017, pp. 65–68.

[9] V. Palazzi, C. Kalialakis, F. Alimenti, P. Mezzanotte, L. Roselli, A. Collado, and A. Georgiadis, "Design of a ultra-compact low-power rectenna in paper substrate for energy harvesting in the Wi-Fi band," in *Proc. IEEE Wireless Power Transf. Conf. (WPTC)*, May 2016, pp. 1–4.

[10] V. Palazzi, J. Hester, J. Bito, F. Alimenti, C. Kalialakis, A. Collado, P. Mezzanotte, A. Georgiadis, L. Roselli, and M. M. Tentzeris, "A novel ultra-lightweight multiband rectenna on paper for RF energy harvesting in the next generation LTE bands," *IEEE Trans. Microw. Theory Techn.*, vol. 66, no. 1, pp. 366–379, Jan. 2018.

[11] S.-E. Adami, P. Proynov, G. S. Hilton, G. Yang, C. Zhang, D. Zhu, Y. Li, S. P. Beeby, I. J. Craddock, and B. H. Stark, "A flexible 2.45-GHz power harvesting wristband with net system output from −24.3 dBm of RF power," *IEEE Trans. Microw. Theory Techn.*, vol. 66, no. 1, pp. 380–395, Jan. 2018.

[12] K. Nishida, Y. Taniguchi, K. Kawakami, Y. Homma, H. Mizutani, M. Miyazaki, H. Ikematsu, and N. Shinohara, "5.8 GHz high sensitivity rectenna array," in *IEEE MTT-S Int. Microw. Symp. Dig.*, May 2011, pp. 19–22.

[13] G.-L. Zhu, J.-X. Du, X.-X. Yang, Y.-G. Zhou, and S. Gao, "Dual-polarized communication rectenna array for simultaneous wireless information and power transmission," *IEEE Access*, vol. 7, pp. 141978–141986, 2019.

[14] W.-H. Tu, S.-H. Hsu, and K. Chang, "Compact 5.8-GHz rectenna using stepped-impedance dipole antenna," *IEEE Antennas Wireless Propag. Lett.*, vol. 6, pp. 282–284, 2007.

[15] A. Z. Ashoor, T. S. Almoneef, and O. M. Ramahi, "A planar dipole array surface for electromagnetic energy harvesting and wireless power transfer," *IEEE Trans. Microw. Theory Techn.*, vol. 66, no. 3, pp. 1553–1560, Mar. 2018.

[16] S. Shen, C.-Y. Chiu, and R. D. Murch, "Multiport pixel rectenna for ambient RF energy harvesting," *IEEE Trans. Antennas Propag.*, vol. 66, no. 2, pp. 644–656, Feb. 2018.

[17] Y.-Y. Hu, S. Sun, H. Xu, and H. Sun, "Grid-array rectenna with wide angle coverage for effectively harvesting RF energy of low power density," *IEEE Trans. Microw. Theory Techn.*, vol. 67, no. 1, pp. 402–413, Jan. 2019.

[18] E. Vandelle, D. H. N. Bui, T.-P. Vuong, G. Ardila, K. Wu, and S. Hemour, "Harvesting ambient RF energy efficiently with optimal angular coverage," *IEEE Trans. Antennas Propag.*, vol. 67, no. 3, pp. 1862–1873, Mar. 2019.

[19] S. Chandravanshi, S. S. Sarma, and M. J. Akhtar, "Design of triple band differential rectenna for RF energy harvesting," *IEEE Trans. Antennas Propag.*, vol. 66, no. 6, pp. 2716–2726, Jun. 2018.

[20] S. Shen, C.-Y. Chiu, and R. D. Murch, "A dual-port triple-band L-probe microstrip patch rectenna for ambient RF energy harvesting," *IEEE Antennas Wireless Propag. Lett.*, vol. 16, pp. 3071–3074, 2017.

[21] S. Chandravanshi and M. J. Akhtar, "An efficient dual-band rectenna using symmetrical rectifying circuit and slotted monopole antenna array," *Int. J. RF Microw. Comput.-Aided Eng.*, vol. 30, no. 4, Apr. 2020, Art. no. e22117.

[22] S. Chandravanshi, K. K. Katare, and M. J. Akhtar, "Broadband integrated rectenna using differential rectifier and hybrid coupler," *IET Microw., Antennas Propag.*, vol. 14, no. 12, pp. 1384–1395, Oct. 2020.

[23] U. Olgun, J. L. Volakis, and C.-C. Chen, "Design of an efficient ambient WiFi energy harvesting system," *IET Microw., Antennas Propag.*, vol. 6, no. 11, pp. 1200–1206, Aug. 2012.

**SANDHYA CHANDRAVANSHI** (Member, IEEE) received the B.Tech. degree in electronics and communication engineering from Madan Mohan Malviya Engineering College, Gorakhpur, India, in 2009, the M.Tech. degree in VLSI design from Banasthali Vidyapith, India, in 2013, and the Ph.D. degree in materials science program from the IIT Kanpur, Kanpur, India, in 2020. From 2009 to 2011, she was a Lecturer with the Prabhat Engineering College, Kanpur. In 2019, she joined the Institute of Electronics, Communications and Information Technology, Queen's University Belfast, Belfast, U.K., where she is currently a Research Fellow. Her current research interests include RF energy harvesting, RF circuits, wireless power transfer, rectennas, metasurface, and compact antenna.

**KRANTI KUMAR KATARE** (Member, IEEE) received the M.Tech. degree from the Electronics Department, IIT (BHU), Varanasi, India, in 2013, and the Ph.D. degree in electrical engineering from IIT Kanpur, India, in 2020. From 2013 to 2014, he worked as an Assistant Professor with Galgotias University, Greater Noida, India. He is currently working as a Postdoctoral Research Fellow with Lund University, Sweden, in association with Volvo Car Corporation, Sweden. His research interests include vehicular antennas, V2X communication, microwave antennas, metasurface inspired antennas, directive array based antennas, partially reflecting surface, artificial magnetic conductor, and RF energy harvesting.

**M. J. AKHTAR** (Senior Member, IEEE) received the Ph.D. degree in electrical engineering from Otto von Guericke University Magdeburg, Magdeburg, Germany, in 2003. From 1994 to 1997, he was a Scientist with the Central Electronics Engineering Research Institute, Pilani, India, where he was involved in the design and development of high power microwave tubes. From 2003 to 2009, he was a Postdoctoral Research Scientist and a Project Leader with the Institute for Pulsed Power and Microwave Technology, Karlsruhe Institute of Technology, Karlsruhe, Germany, where he was involved in a number of projects in the field of microwave material processing. In 2009, he joined the Department of Electrical Engineering, IIT Kanpur, Kanpur, India, where he is currently a Professor. He has authored two books, two book chapters, and has authored or coauthored more than 200 papers in various peer-reviewed international journals and conference proceedings. He holds two patents on RF sensors for testing of solid and liquid sample, and one patent on nanomaterial integrated RF sensor for detection of harmful gases in the environment. His current research interests include RF, microwave and THz imaging, microwave nondestructive testing, metamaterial inspired RF sensors, SIW based RF devices and sensors, RF energy harvesting, plasmonic devices, functional materials, wideband electromagnetic absorbers, UWB antennas for imaging, and design of RF filters and components using the electromagnetic inverse scattering. He is a Fellow of the Institution of Electronics and Telecommunication Engineers, New Delhi, India, and a Life Member of the Indian Physics Association and the Indo-French Technical Association. He was a recipient of the CST University Publication Award from the CST AG, Darmstadt, Germany, in 2009. He served as the Chair for the IEEE Microwave Theory and Techniques Society Uttar Pradesh Chapter from 2013 to 2015, and the Vice-Chair for the IEEE Uttar Pradesh Section in 2015.